Biometrics Retinal Identification System and Iris Recognition

Avinash Yadav
Student
Department of Information Technology
Institute of Engineering & Technology - Dr. RML Avadh University, Ayodhya, Uttar Pradesh, India

Samriddhi Singh
Assistant Professor
Department of Information Technology
Institute of Engineering & Technology - Dr. RML Avadh University, Ayodhya, Uttar Pradesh, India

Abstract

A biometric system provides automatic identification of an individual based on a unique feature or feature that the person possesses. Unlike other biometric such as fingerprints and facial recognition, the distinct aspect of the iris comes from randomly distributed features. Iris recognition is considered to be the most reliable and accurate biometric detection system available. In this paper, I describe novel techniques developed to provide an iris recognition system. This paper proposes an individual identification using iris recognition system with the help of six major steps i.e. image acquisition, localization, isolation, normalization, feature extraction and matching and several small steps to complete each step in these six steps are included. Iris boundaries are detected using the canny edge detector and circular hoop transformations, as the papillary and limbic boundary. We can use masking technique to isolate the iris image, separate the given eye image, this separate iris image changes from Cartesian to Polar Coordinate. Now finally extract the unique features of the iris (feature vector) after enlarging the iris image and then perform matching process on the iris code using the Hamming distance for the acceptance and rejection process. I am giving my review after studying many research papers and my proposed technique works very well and can be implemented easily.

Keywords- Biometrics Identification & Technology, Iris Recognition, Edge Detection, Transformation, Masking, Feature Vector, Hamming Distance

I. INTRODUCTION

Now-a-days, one of the main threats to the IT system and security environment, is the possibility of intruders in the system. This is usually solved by user authentication schemes based on passwords, secret codes and identity cards or tokens. Schemes based only on passwords or secret codes can be prevented by stopping the presentation of such passwords or by brute force attacks. On the other hand, an intruder can attack the system based on identity cards or tokens, loot them, copy or emulate them. As it is a well-known, biometric deal, individuals are identified based on their physical and behavioral characteristics.

Identification systems using biometric solutions, such as fingerprint, iris, face, and palm print, hand geometry, signature, etc.; There are many advantages over traditional authentication techniques, depending on what you know or what you have. Instead of carrying a bunk of keys, all the access cards or passwords you carry with you can be used to identify your body uniquely. Among them, iris recognition is tested as the most accurate method of personal identification. So nowadays many automated security systems based on iris recognition are deployed around the world for border control, restricted access etc.

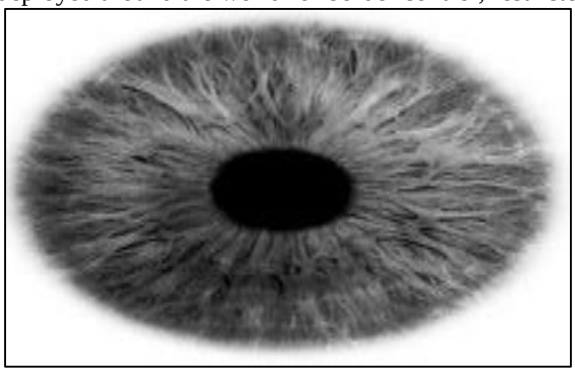

Fig. 1: Rich Iris Picture

This technique identifies better than other biometric identities because I am using an iris that has an exceptional structure and provides many interlocking minute features such as freckles, coronas, strips, furrow, and crypts etc. These visible features, commonly called iris design, are unique to each subject. The iris patterns of two eyes of an individual or identical twins are completely independent and unrelated. All biometric systems suffer from two types of errors in the form of false acceptance and false rejections. But the iris recognition system gives us a lower false acceptance and false rejection rate than any other individual

recognition system because the iris is preserved behind the eyelid, cornea and aqueous, meaning that unlike other biometrics such as fingerprints, The probability of damage is minimal, the iris is also not subject to the effects of aging, meaning that it remains stable from about one year of age until death. Therefore we do not need to update the database repeatedly. Thus the entire system is giving us maximum accuracy and low error rate for personal identification in biometric analysis.

II. RETINAL TECHNOLOGY

A. Retina Anatomy

Figure 2 shows a lateral view of the eye. The retina is about 0.5 mm thick and covers the posterior side of the eye. The center of the retina consists of an optical nerve or optical disc (OD), which is about 2 × 1.5 mm (about 1/30 of the retinal diameter), of a spherical oval white area. The blood vessels are continuous patterns with little curvature, branching from the OD and the shape of the tree on the surface of the retina (Figure 3). The average diameter of the vessels is approximately 250 μm (1/40 of the retinal diameter)

The retina is essentially a sensory tissue consisting of several layers. There are also literally millions of photoreceptors in the retina, whose function is to collect the light rays that are sent to it and convert that light into electrical impulses that travel through the optic nerve in the brain, which later these impulses convert it into images. The types of photoreceptors present within the retina are called rods and cones. Cone (there are about 6 million cones)

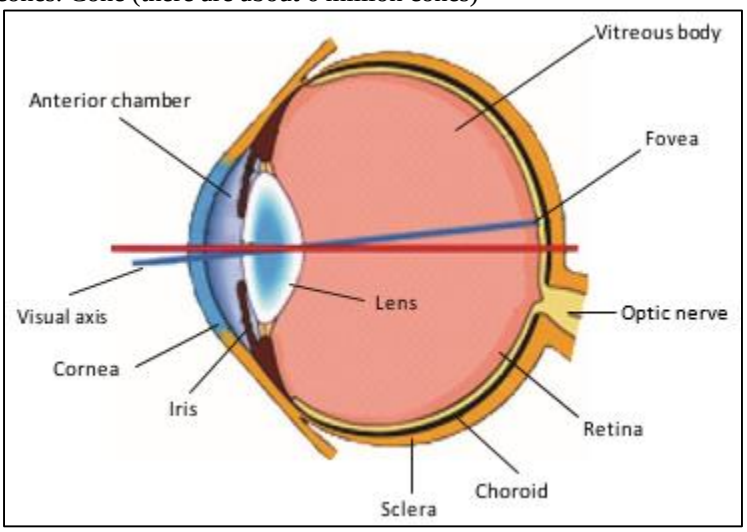

Fig. 2: Eye Anatomy

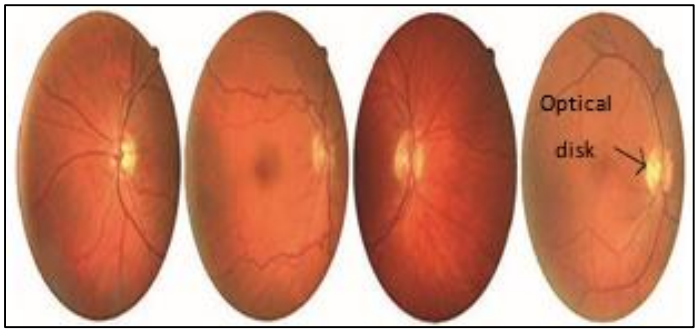

Fig. 3: Retina images of four different subjects

Help us see different colors, and there are sticks (about 125 million sticks) with night and peripheral vision.

B. How can Retinal Anatomy be used to Identify People?

When the eye is talked about, especially in the context of biometrics, there is often confusion between the iris and the retina of the eye, in which the two are similar. While the iris and retina can be placed together in a broad category called "eye biometrics", the function of the two is completely different. The iris is the colored area between the pupil and the white area of the eye (also called the sclera). The primary role of the iris is to dilute and constrict the size of the pupil. As shown in Figure 2, the iris is located in front of the eye, and the retina is located in the back of the eye. Because of its internal position within the eye, the retina is not in contact with the external environment, and thus it possesses a very stable biometric. It is the blood vessel pattern in the retina that forms the basis for the science and technology of retinal detection. Figure 3 shows different retinas from four people.

III. SOME CURRENT AND FUTURE APPLICATIONS

Iris recognition systems have a world-wide application area. National border control, in the form of passport, computer login: a password, secure access to bank account in ATM machine, ticketless travel, authentication in networking, permission control for home, office, lab etc. Control, driving license, and other personal Security at the desired person, anti-terrorism, airports, using certificates, missing trace or any type of password.

Fig. 4: Travelers scanning the iris for the security system

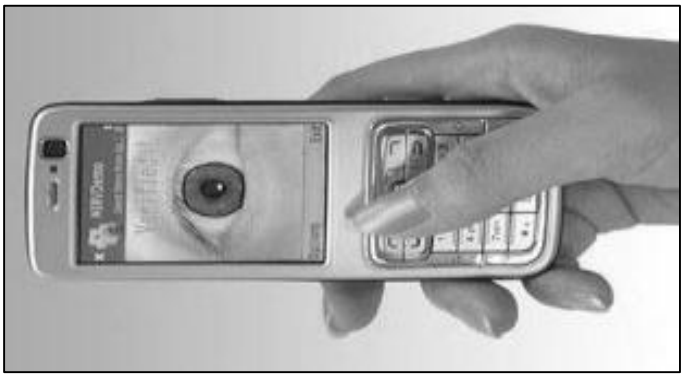

Fig. 5: Mobile Security

Fig. 6: Security check at the border

This paper represents a review of the identity of a person using iris recognition after studying several papers, articles. My paper is organized as follows: background work by several authors, given to the researcher as related work in section II, in my system, how it works, of image capturing, edge detection, internal and external search As for all the major and minor step limits, isolation, polarization from the Cartarian, image enhancement, features extraction and matching, my whole system approach is given in Section III as the iris recognition system, the whole subject and Future work is finally given as a conclusion in Section IV. All the letters and websites that I have used to provide this review are given in section V under heading reference.

IV. RELATED WORK

So many authors present their techniques related to this system, in this system I studied most of the good papers in order. Phloem and Safir first proposed the concept of automatic iris recognition. A report was published by Johansson in 1992 with no experimental results. Since then, iris recognition has been gaining the attention of many researchers and a great deal of progress

has been achieved in the last decade. For example, Daugman realized an iris recognition system and the detection accuracy is up to 98.9%. Dugman proposed an intra-resolution method to find the pupil and iris, which he considered the pupil and iris boundary spherical. Dogman's iris recognition algorithm is based on the principle of failure to test for statistical independence on the iris phase structure encoded by quadrature wavelets. Bolles and Bose Hash computed the zero-crossing representation of a 1-D wavelet transform at different resolution levels of a virtual circle on an iris image to characterize the iris texture. Iris matching was based on two differentiation functions. Wilds represented the iris texture with a Laplacian pyramid constructed with four different resolution levels.

V. IRIS RECOGNITION SYSTEM

When a subject wants to be identified by the iris recognition system, his / her eye is first photographed and then a template (iris code) is created for his or her iris area. This template is then compared with other templates stored in the database, until a mismatch is found and the subject is identified or a mismatch is found and the subject remains unknown. There are many ways to complete a single task in the form of edge detection. I Sobel Operator, Prewitt Operator, Canny Edge Detection, Roberts Method etc. I have phase based methods, zero crossings and texture analysis based methods for feature extraction, algorithms and so on. As per studies by various papers, a well-defined move has come to my mind that may appear to various readers, researchers and is fixed as picture to picture: 7 is given below.

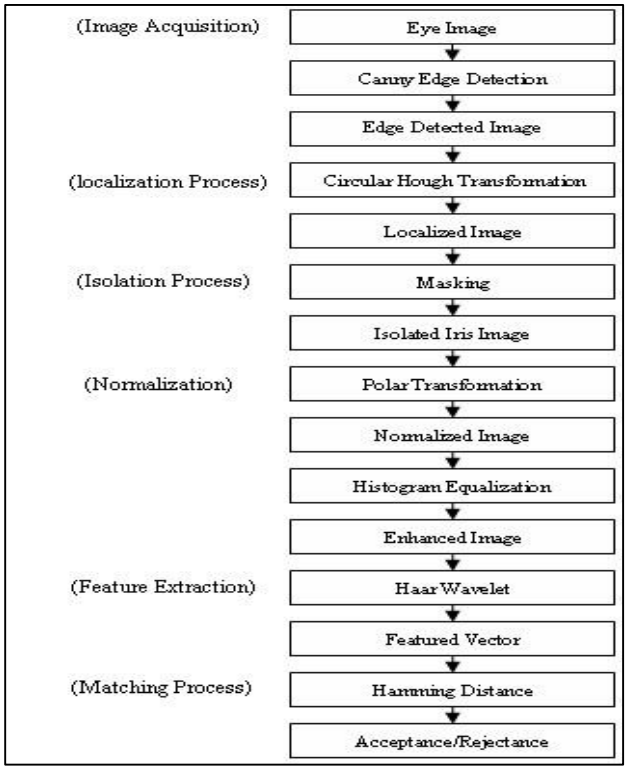

Fig. 7: My System

Figure 8 shows the various parts of our new biometric detection system based on retinal images. As depicted in the block diagram, the system consists of three major modules, including blood vessel segmentation, feature generation, and feature matching. Blood vessel segmentation provides a binary image containing the pattern of blood vessels that will be used by the next module. The feature generation module consists of several submodules: (i) the masking vessel in the vicinity of the OD, (ii) the polarity transform to obtain a rotating invariant binary image consisting of the major retinal vessels, (iii) the resulting binary resulting from the wavelet transform. Multicellular analysis of image. To separate the vessels according to their diameter size, and (iv) feature vector construction from three images, each of which contains vessels with a specified range of diameter sizes. The feature matching module consists of the following submodules: (i) calculation of similarity indices called SI for three different scales, (ii) scale-weighted sum of SI to construct the total SI, and (iii) subject recognition. Thresholding the calculated SI.

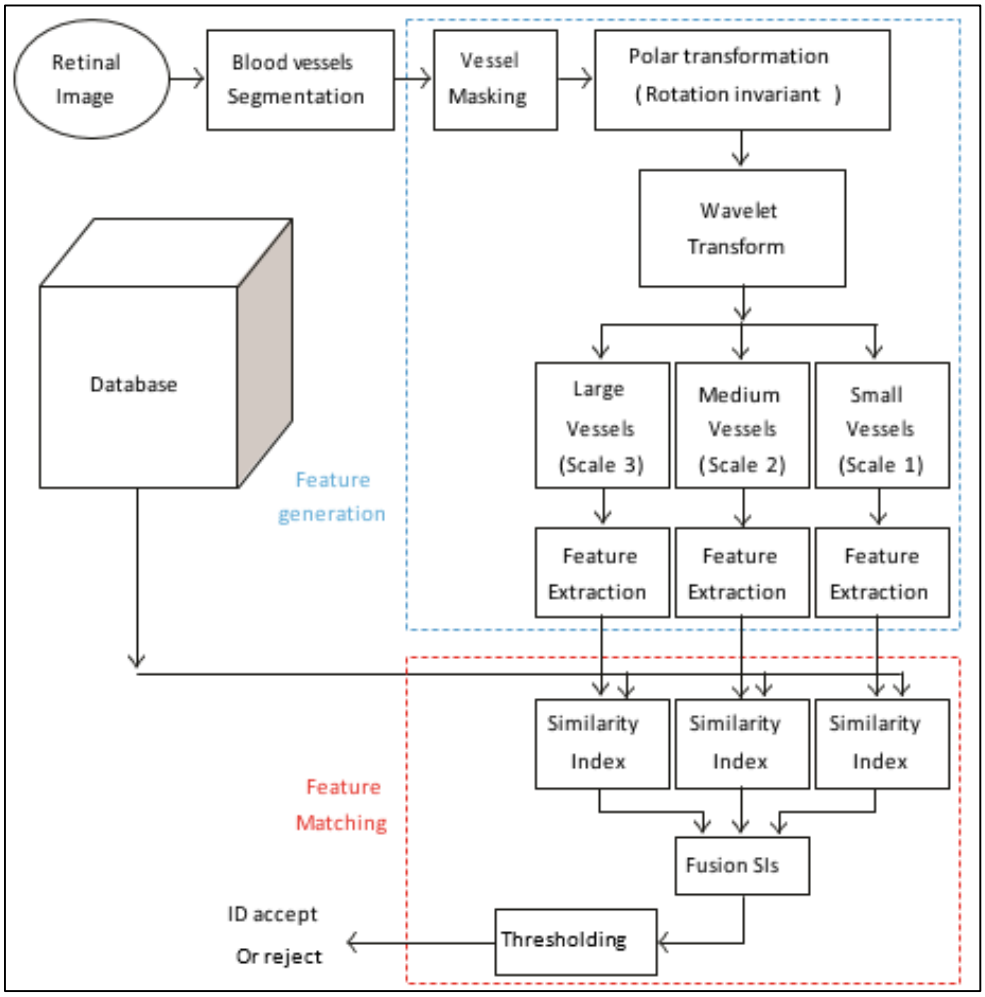

Fig. 8: Retinal Identification System

The primary application for retinal detection has been for physical access entry for high security features. This includes military installations, nuclear facilities and laboratories. In an effort to reduce welfare fraud, one of the best documented use of retina detection was conducted by the state of Illinois. The primary objective was to identify welfare recipients, so that benefits could not be claimed more than once. Iris recognition is also used in conjunction. Retinal imaging is a

(A)

(B)

(C)

(D)

Fig. 9: Some retinal scanners, (A) a human retinal scanner, (B) and (C) human retinal detection scanner, and (D) a cow retinal scanner

The form of identification that can be used in both animals and humans.

VI. IMAGE ACQUISITION

This is our first phase of the entire process. When a person wants to be identified by the iris detection system, his eye is first photographed. The camera can be placed between three and a half inches and a meter to capture the image. In the manual process, the user needs to adjust the camera to bring the iris into focus and must be within six to twelve inches of the camera. This process is much more manually intensive and requires proper user training to succeed. We should consider that iris, lighting, and number of pixels on the iris are factors that affect image quality. Many researchers have used the Chinese Academy of Sciences Institute of Automation and Malaysia Multimedia University (MMU) databases to conduct their research.

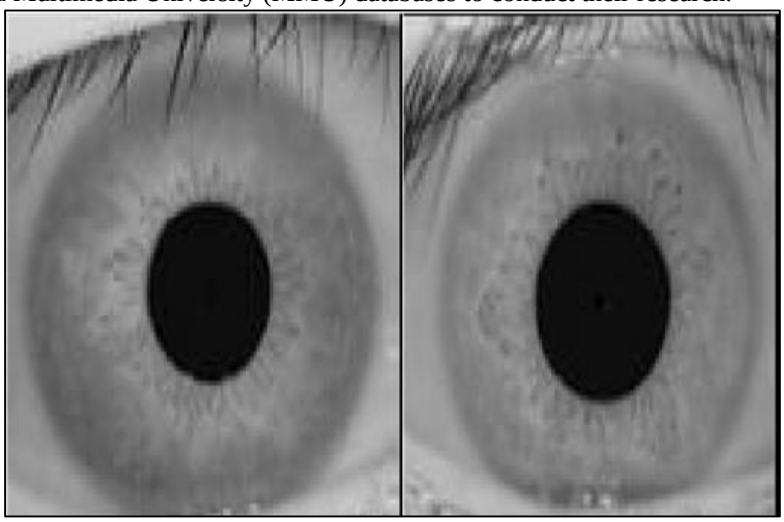

Fig. 10: Sample iris images

VII. LOCALIZATION

In order to detect the iris, the acquired iris image must be preprocessed, which is an annular portion between the pupil (inner border) and the sclera (outer border). The first step in iris localization is the detection of pupil which is a black spherical part surrounded by iris tissue. The center of the pupil can be used to detect the outer radius of the iris pattern. Important steps involved are:

1) Pupil detection
2) External Iris Localization

Famous methods such as integro-

Differential operators, hoop transforms and active contour models have been successful techniques in detecting boundaries. Iris localization proposed by Tiss et al. Is a combination of integro-differential operator and Hof transform. The Hoff transform is used for quick approximation of the pupil center and then the Integro Difficiency operator is used to accurately locate the pupil and limbus using a small search space. But in this paper I am using canny edge detection to detect edges in the image of the entire eye, followed by applying circular shock changes to detect the outer border of the iris using the pupil center and the inner border of the iris do.

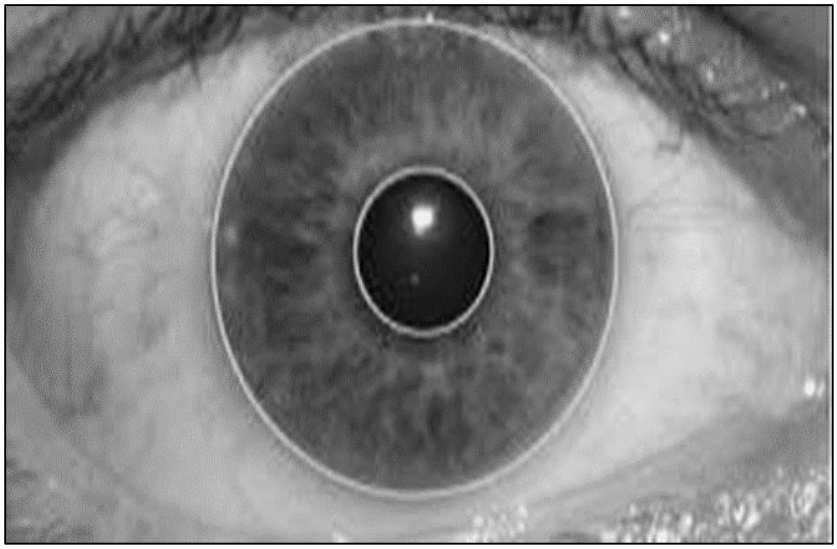

Fig. 11: Localized Iris Image

VIII. ISOLATION

Now the task is to separate the iris. In the images used, the eye has some presence of white. This was done using a masking technique because here I am choosing the best technique among others so I will use a Gaussian mask and then crop the image to reduce the area that has no edge data. . The mask is a sphere with the same radius as the iris. It thus encircles all the pixels that are all pixels that make up the iris. Using the center and radius that are calculated at the advanced stage, we set the polar coordinate system. In this coordinate system, the characteristic of the iris is extracted.

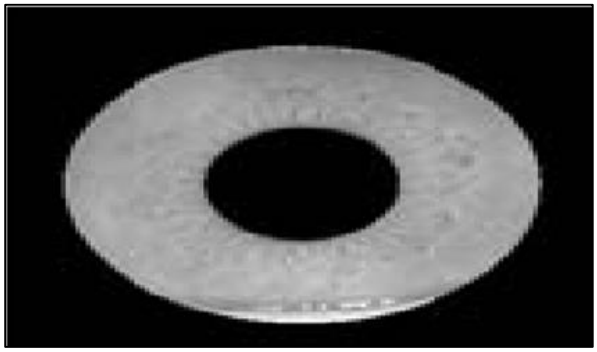

Fig. 12: Isolated iris image

IX. NORMALIZATION

For the purpose of precise texture analysis, it is necessary to compensate for this distortion. Since both the internal and external boundaries of the iris are explored, it is easy to map the iris ring into a rectangular block of a fixed-size texture. The Cartesian for polar reference transformation suggested by Dogman denotes a rectangular representation equal to the region of interest as shown. In this way I compensate for the stretching of the iris texture as the pupil changes in size, and the next feature reveals the frequency information contained in the circular texture to facilitate extraction. Also this process is very essential as the feature extraction and matching process becomes easier.

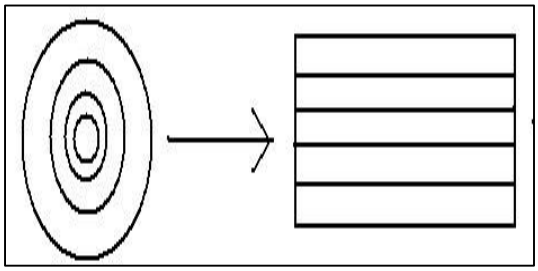

Fig. 13: It shows how the iris is converted to polar coordinates

Thus the following set of equations is used to convert the annular region of the iris to its polar counterpart. I (x (ρ, θ), y (ρ, =) => I (ρ, p) xp (ρ, θ) = xp0 (θ) + rp * cos (θ) yp (ρ, θ) = yp0 With (θ) + rp * sin (θ) xi (ρ), r) = xi0 (i) + Ri * cos (θ) Yi (ρ, θ) = yi0 (θ) + Ri * sin (θ)

Where, Rp and Ri are the radii of the pupil and the iris, respectively, while (xp (p), yp (y) and (xi (,), yi (θ)) are the coordinates of the papillary and limbic boundaries. The value of the direction θ. Θ. [Relates to 0; 2], ρ [Relates to 0; 1].

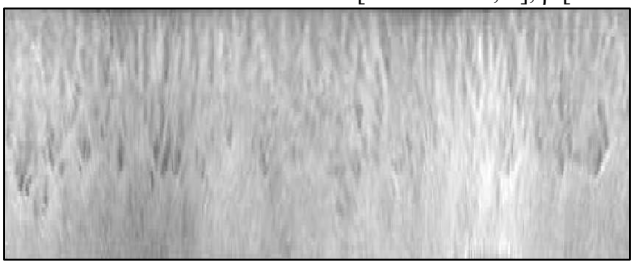

Fig. 14: Unrelated image

X. ENHANCEMENT AND CONDEMNATION

The normalized iris image still has low contrast and can cause non-uniform illumination due to the position of the light sources. To obtain a more well-distributed texture image, we enhance the iris image through the local histogram equation and remove the high frequency noise by filtering the image with a suitable filter.

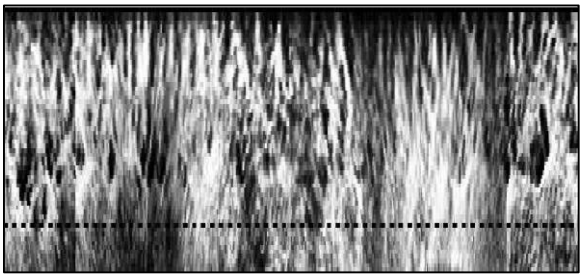

Fig. 15: Iris image after development and sensor

A. Local Contrast Development

In the local processing operation, a sliding window of M × M (M is at least 50 times smaller than the dimensions of the original image) is used to obtain a contrast-enhanced image. In each pixel, the new value is calculated using the version / version of the window values and the global maximum / minimum values in the original image. Let the value of pixel (i, j) be f (i, j) in the original image. The augmented image g (i, j) is calculated according to the following equations.

(1)

$$f(i,j) \longrightarrow g(i,j) = \frac{H - W_{\text{Min}}}{W_{\text{Max}} - W_{\text{Min}}},$$

$$H = \frac{1}{\text{Mean} + (1 \quad / \quad \sqrt{\text{var}})\exp \quad - \quad \text{Mean} \quad - \quad f(i,j) \quad ^{0.98} / \quad \sqrt{\text{var}}},$$

$$W_{\text{Min}} = \frac{\text{Mean}}{1 + \exp \quad - \quad \text{Mean} \quad - \quad f_{\text{min}} \quad / \quad \sqrt{\text{var}}},$$

$$W_{\text{Max}} = \frac{\text{Mean}}{1 + \exp \quad - \quad \text{Mean} \quad - \quad f_{\text{Max}} \quad / \quad \sqrt{\text{Var}}},$$

Fig. 16: Local contrast enhanced image

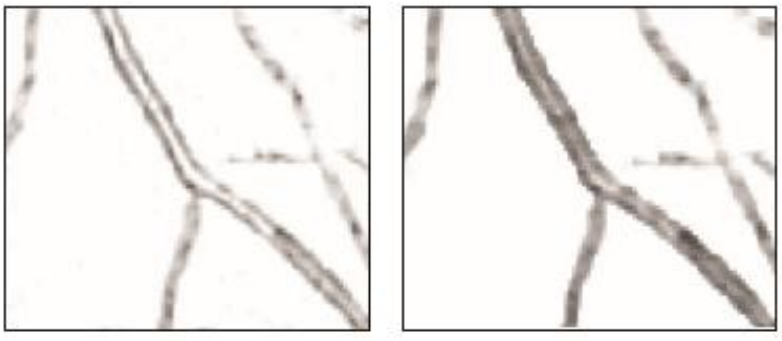

(a) (b)

Fig. 17: Morphological correction: (A) vessels after contrast enhancement, (B) vessels after morphological correction

Where var and mean are variances and mean values inside the window, and fmin and fmax are the minimum and maximum of the global green plan image, respectively. It is clear that H is a mapping function from f to g. Figure 16 local contrast Growth image.

B. Morphological Enhancement

Following the local contrast enhancement process, we encounter a problem that transforms large vessels into two parallel curves as depicted in fig. 17 (a). This problem is caused by the smaller size of the selected window (in the previous step) than the size of the larger vessels. To solve this problem without modifying the thickness of the vessels, we use morphological dispersion and erosion to fill in the blanks between two parallel curves. Figure 17 (b) shows the larger vessel in Figure 17 (a) after morphological correction.

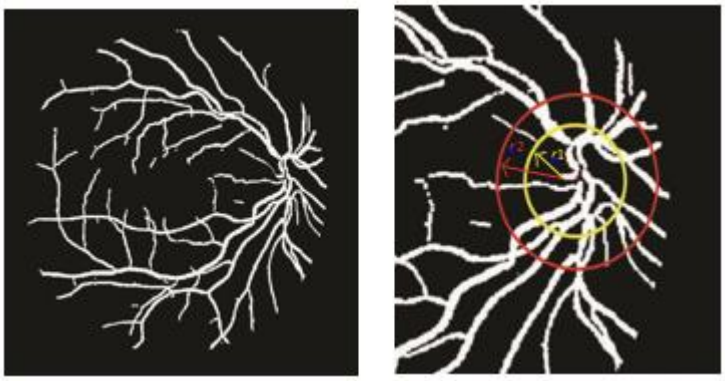

(a) (b)

Fig. 18: Blood splitting and masking: (a) pattern of vessels, (b) area of images of vessels around OD

XI. FEATURE EXTRACTION

Lim et al. Also use wave transformation to remove features from the iris area. Both Gabor metamorphism and each wavelet are considered to be mother wavelets. Laplacian of Gaussian (LoG) is also used in previous papers. In my paper, using every wavelet, a feature vector with 87 dimensions is computed by decomposing it to the fourth level. Since each dimension has a real value from -1.0 to +1.0, the feature vector is indicated in a quantity so that any positive value is represented by 1 and a negative value. 0. This results in a compact biometric template with only 87 bits.

XII. FACILITY CREATION

Our retinal detection system uses the features of blood vessels patterns, including their diameter and their relative locations and angles. To generate these features, the algorithm uses the four submodules summarized in Section 2.1. A detailed description of these submodels is given in the following sub-sections.

A. Vessel Masking

Vessels around OD are more important for identification purposes because there is less randomness within a subject in their distribution pattern around OD. In other words, as vessels are moved away from the OD, they become thinner and their distribution is more random such that it has a less discriminating property. Therefore, the OD location can be used as a reference point for the position of the human eye in relation to the scanner system. This means that the OD must be placed in the central region of the scanned image to allow the detection to be performed. After evacuating the vessels and localizing the OD by the vessel division algorithm, we focus on the vessels around the OD. A ring mask centered on the OD location with Ready r1 and r2 (r1 <r2) is used to select the ROI in the vessel-segmented binary image (Figure 18 (b). This binary ROI is used in the next steps Is done for feature generation.

B. Polar Change and Rotation Invitation

Images of the retina from the same subject from the eye and head movements in front of the scanner may have some degree of rotation. Therefore, rotation invariant features are necessary to prevent detection errors due to the rotation of the image. This is why we use polarity transforms to obtain a rotating inductive binary image consisting of retinal vessels in the vicinity of the OD. The polar image can be constructed by following changes from Cartesian coordinates. The point (x, y) in Cartesian coordinates is the point in polar coordinates $\rho = (x2 + y2)$, changed to ct = arctg (y / x). A polar image made from the ROI image is shown in Figure 19. The polar image is 30 × 360 in size with the second dimension referring to viewing angle of ROI.

C. Multicellular Analysis of Polar Image

Diameter sizes vary in the vicinity of the OD. This property can be used as the first feature in a feature generation module. In this way, a human observer can simulate mental activity in multicellular analysis of any polar image. In other words, a human observer classifies the areas around the OD into large, medium and small, and uses their relative positions to identify each individual. For

this purpose, we analyze the polar image in three scales through discrete stationary biorothogonal wavelet transforms. Obviously, alternative methods such as image processing can be used to determine the diameter of vessels. However, the diameter non-symmetry of each vessel in the polar image can complicate such an approach (Fig. 20 (see B)). Figure 20 (a) shows that the residual coefficient resulted from applying the wavelet transform in the polar image in Figure 19 (b) to the first three scales. To extract larger vessels from the polar image, we limit the residual coefficient in the third scale of the wavelet transform. To extract medium-sized vessels, we remove larger vessels from the polar image and repeat the same procedure on the residual coefficient of wavelet transformation in the second scale. Finally, we remove large and medium-sized vessels from the polar image to obtain smaller vessels. The result of the vessel separation process is depicted in Figure 20 (b).

D. Feature Vector Creation

Figure 19 shows how a vector is constructed using a vectors decomposed polar image. To construct the feature vector, we localize the vessels in each scale and replace them with rectangular pulses. The duration of each pulse is experimentally fixed at 3 points, and its amplitude is equal to the angle between the respective vessel orientation and the horizontal axis. Therefore, the final attribute vector is composed of 3 vectors (on a scale), each with 360 values. Clearly, the zero value in each vector corresponds to the noncell positions in the waveform decomposed polar image. Further consideration should be given to the memory size required for each feature vector. One can reduce the redundancy of feature vectors by using run length coding (RLC). This coding may reduce the average size of the feature

(A) (b)

Fig. 19: Polar transform: (a) ROI in Cartesian coordinates, (b) polar image

(A) (b)

Fig. 20: (a) Multicellular analysis of the polar image: wavelet approximation coefficients in scale 3 (top), 2 (middle), and 1 (bottom); (B) Ship separation results: large (top), medium (middle), and small (bottom) vessels

The vectors range from 3 × 360 bytes to only 3 × 48 bytes, which is much smaller than the 256 bytes for the iris code.

XIII. STORAGE AND MATCHING

Now this is the final step to complete our system. Here we will store 87 bit iris code or template in our database for future matching and this matching is done with the help of an efficient matching algorithm, which we are using to identify two samples in the Hemming Distem algorithm. Templates which are reference templates and nomination. It basically uses a special OR (XOR) function between two bit patterns. Hamming distance is a measure that delineates differences in iris codes. Each bit of the presented iris code is compared to each bit of the referenced iris code if the two bits are the same, e.g. Two 1 system s or two 0, s, the system provides a value for 0 for that comparison and if the two bits are different, the system provides a value 1 1 for that comparison. The formula for iris matching is shown as follows:

HD = 1 / N = (Pi Ri) [13] Where N is the dimension of the feature vector, Pi is the ith component of the presented feature vector while Ri is the ith component of the referenced feature vector.

Here we can set a threshold value if the resulting value is greater than the threshold value, reject the iris and the user accepts the iris.

According to the review, I am giving my views on the matching process, which can be stored in the figure and represented by a diagram called the matching process: 12.

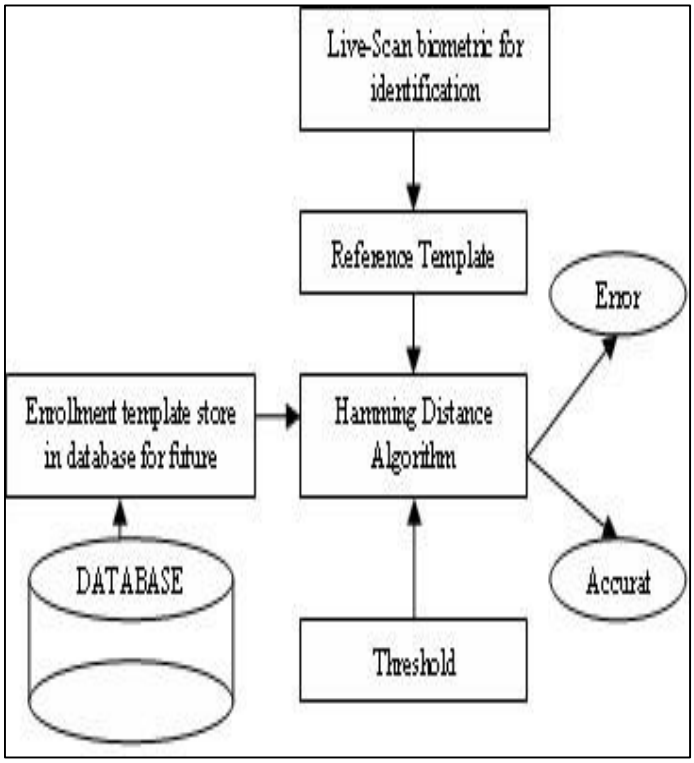

Fig. 21: Storage and matching process

For feature matching, we introduce a new similarity index based on a modified correlation between feature vectors. The modified correlation (MC) between the two feature vectors for the ith scale is defined as follows:

(2)

$$MC_i(\varphi) = \sum_{\tau=} \text{step}\theta_i(\tau) \times \theta_i^q(\tau + \phi) * \cos[\alpha \times (\theta_i(\tau) - \theta_i^q(\tau + \varphi) \quad , \quad i = 1,2,3,$$

Where θi is the feature vector corresponding to the named image, and αiq is the feature vector corresponding to the input query image, α 1.7 has a coefficient set experimentally, circular represents the circular translation value, and N = 360 is the length of each scale. Vector feature in The step (·) step function is defined as follows:

1, x> 0,

Step (x) = ≤ (3)

0, x 0.

The role of phase (·) in (2) is to normalize the product of pulse amplitudes in feature vectors, since the amplitude of each pulse specifies the orientation of the respective vessel and is used only to determine the logic of cos (·). Is done for two). The role of cos (·) in (2) is to take into account the angle between the vessels in the named and query images. Since the angle between ships is rarely greater than 90 degrees, we use a coefficient α (between = 2) in the logic of cos (·) to reduce the modified correlation value, when ships are given a Is not oriented in the same direction. If two ships have the same orientation, the angle between them will approach zero and cos (·). Will assume close to 1. Conversely, if they are oriented differently (eg, about 90 degrees), then the angle between them will be different from zero and will go to cos (·) and1. The similarity index between the named and query image on the ith scale is defined as the maximum value of the modified correlation function:

SI = Max MCI (ϕ), i = 1,2,3. (4) 4 = 1, ..., 360

Finally, a scale-weighted sum of SIs is computed to obtain the total SI for enrollment and query images. In general, larger vessels are more effective than smaller ones for identification. Therefore, we used three different weights (w1> w2> w3) to obtain a weighted sum of the parity indices:

SI = w1 × SI1 + w2 × SI2 + w3 × SI3,

Where SI is the total similarity index used for identification. In this work, we used the following experimental weights: w1 = 2.0, w2 = 1.5, and w3 = 0.5.

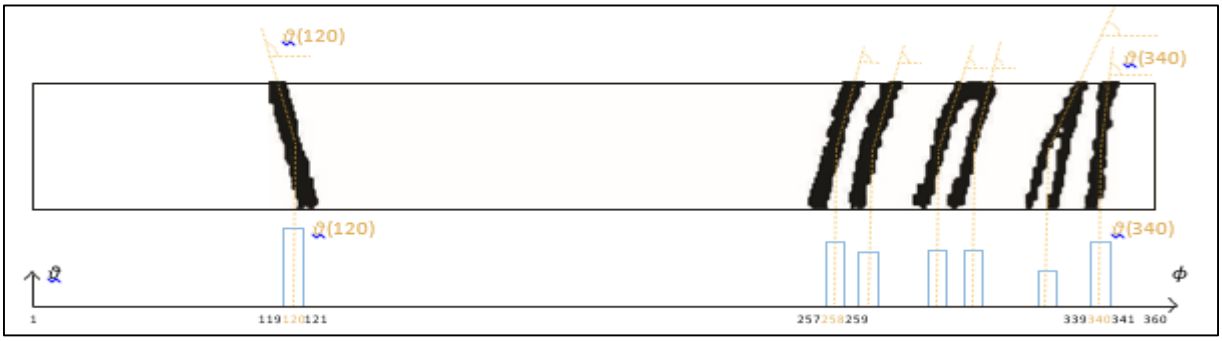

Fig. 22: Construction of feature vector in the second scale (medium-size vessels), the horizontal axis, shows the position of vessels (in degrees) in polar coordinates and the vertical axis and shows the angle (in degrees) between corresponding vessel orientation and the horizontal axis in the polar image

Table 1: Experimental results

Experiment	*Experiment A*	*Experiment B*	*Experiment C*	*Experiment D*	*Mean*	*Variance*
Accuracy	*99.4%*	*97.9%*	*98.9%*	*99.6%*	*99.0%*	*0.58*

XIV. EXPERIMENTAL RESULTS

We implemented a database including 60 subjects on a single database, 40 images from DRIVE, and 20 images from the STARE database. We randomly rotated each image 5 times to obtain 300 images. We evaluated the performance of our detection system in four different experiments.

A. Experiment A

The first 30 images of the DRIVE database were enrolled, and 60 images of the DRIVE and STARE databases with 5 images per subject were entered into the system for questions.

B. Experiment B

The final 30 images of the DRIVE database were enrolled, and 60 images of the DRIVE and STARE databases with 5 images per subject were entered into the system for questions.

C. Experiment C

The first 10 images from the DRIVE database and the first 10 images from the STARE database were enrolled, and 60 images with 5 images per subject from the DRIVE and STARE databases were entered into the system as queries.

D. Experiment D

The first 15 images of the DRIVE database and the last 15 images of the STARE database were enrolled, and 60 images of the DRIVE and STARE databases were recorded as questions in the system with 5 questions per subject.

These experiments demonstrated that the average accuracy of our system is equal to 99.0 percent. Table 1 shows the results of each experiment. Fig. 23 shows the variation of FRR and FAR according to the distribution of nonmatching distances by selecting the appropriate distance range. Me too

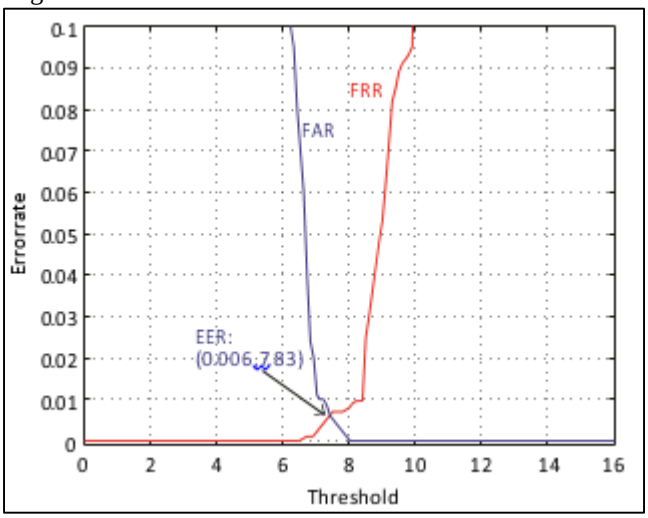

Fig. 23: Difference of FRR and FAR diagram shows EER for experiment with α = 1.7

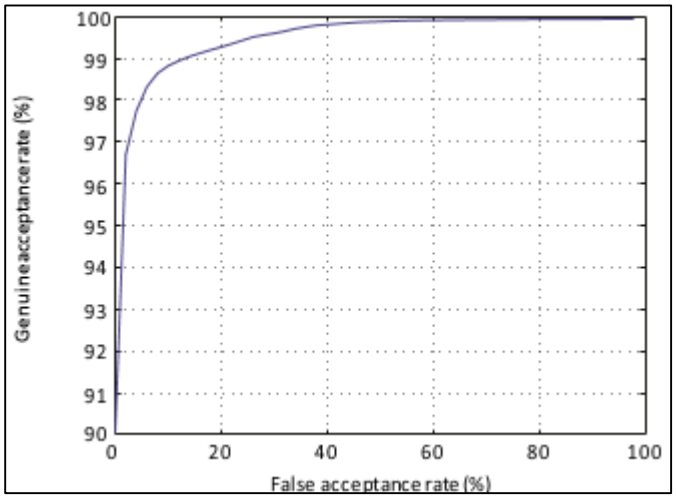

Fig. 24: ROC curve

Figure 24, the ROC curve shows that the large values of the true acceptance rate we have for detection are in very low false acceptance rates.

XV. THE CONCLUSION

In this review paper I show that a person can be identified in many ways, but instead of carrying a keystroke or remembering things as a password, we can use us as a live password, Which is a biometric call recognition technique that uses physical characteristics or habits. To identify any individual, we have many features in biometrics that we are using in our identification technology such as fingerprint, palm print, signature, face, iris recognition, thumb print and so on, but any of them Also identifying the person is the best technique. I can say that this technology is not fully developed and we need many scientists, researchers and developers who can work on this technology and fulfill Mr. Dogman's dream by implementing the use of iris recognition in every field Where security is required by humans.

The primary results obtained by our retinal detection system demonstrate its ability to be used as a reliable biometric system. Further enhancements to our retina detection system can be provided by:

1) Most of the parameters used in the algorithm are experimentally selected to achieve good results. These parameters, such as the weights used in the matching process, can be adapted to provide high average accuracy;
2) The effect of the position of the optical disc within the retinal image can be reduced by performing a general change that brings the OD to the center of the retinal image. In this way, the resulting retinal codes will be less sensitive to the OD position within the retinal image.

REFERENCES

[1] http://www.amazingincredible.com/show/82-the-incredible-human-eye(last referenced April 2013)
[2] P. W. Hellinan, "Recognizing the Human Eye", Geometric Methods Comput. Vision, vol. 1570, pp.21–226, 1991
[3] J. Dogman & c. Downing, "Epigenetic randomness, complexity, and eccentricity of human iris patterns," Proc. Royal Society (London) B: Biological Sciences, Vol. 268, pp. 1737–1740, 2001.
[4] R. Wills, J. Asmuth, G. Green, S. Hue., R. Koloczynski, J. Matty, s. McBride, "A Machine-Vision System for Iris Recognition," Vol. 9, pp.18, 1996.
[5] R. P. Wilds, "Iris Recognition: An Emerging Biometric Technology," Proceedings of the IEEE, sept. Vol.85, pp.1348–1363, 1997.
[6] http://www.cl.cam.ac.uk/~jgd1000/applics.html (Final report 26 April 2013)
[7] http://www.forbes.com/global/2010/04/0412/entrepreneurs-hector-hoyos-iris-scanners-identity-we-see-you.html (last referenced 26 April 2013)
[8] http://pinktentacle.com/2006/11/iris recognition-technology-mobile-phone / (Last referenced 26 April 2013)
[9] L. Flom and A. Safir, "Iris Recognition System," U.S. Patent, No. 4641394, 1987.
[10] a. Bertillon. La Kapoor de Piris. "Scientific Review," Vol. 36, no. 3, pp. 65–73, 1885.
[11] J.G. Dugman, "High-confidence visual recognition of individuals by examination of statistical independence," IEEE Trans. Pattern Anal. Mach. Intelligence, Vol. 15, No. 11, pp.148–1161, 1993.
[12] W. Bolles and B. Bose Hash, "A Human Detection Technique Using Images of Iris Trans and Islets," EE Trans. On Signal Processing, Vol. 46, no. 4, pp.185–1188, 1998.
[13] Kevin W. Bowyer, Karen Hallingsworth, Patrick J. Flynn, "Iris Understanding for Iris Biometrics: A Survey, Computer Vision and Image Understanding," Vol. 110, issue 2, pp. 281–307, 2008
[14] http://www.idealtest.org/dbDetailForUser.do?id=4 (Last referenced 26 April 2013)
[15] http://pesona.mmu.edu.my/~ccteo/ (Last referenced 26 April 2013)
[16] Li Ma, Yunhong Wang, TNIU Tan, "Iris Recognition with Circular Symmetric Filters," National Recruitment of Pattern Recognition, Institute of Automation, Chinese Academy of Sciences, PR China.
[17] c. Tit Martin L. Torres and M. Robert, "Person Identification Technique Using Human Iris Recognition," Proc Vision, pp. 294–299, 2002.
[18] S. Lim, K. Lee, O. Byon, T. Kim, "Efficient Iris Recognition through Improvement of Feature Vectors and Classifiers," ETRI Journal, Korea, Vol. 23, no. 2, 2001.

[19] C. Simon and I. Goldstein, "A New Scientific Method of Identification," New York State Journal of Medicine, vol. 35, no. 18, pp. 901–906, 1935.
[20] H. Book, a. In Proceedings of the Second IEEE International Conference on Information and Communications Technology (ICTTA '06, pp. 1031-1037, Damascus), Milani Fard, and H.W. Jafrani, "A novel human identifier system using retinal image and fuzzy clustering approach". Syria, April 2007
[21] http://www.retica.com/index.html
[22] Medical Data Mining and Knowledge Discovery, PP. 1, 1-212, Springer, Berlin, Germany, 2000. Yes. Goh, W. H. And m. Lee.
[23] S. Chaudhary, s. Chatterjee, N. Katz, M. Nelson, and M. Goldbom, "Detection of blood vessels in retinal images using two-dimensional matched filters," IEEE Transactions on Medical Imaging. 8, no. 3, pp. 263–269, 1989.
[24] Http://www.raycosecurity.com/biometrics/EyeDentify.html
[25] W.-S. Chen, K. H. Chih, S.W. Shih, and C.-M. Hsieh, "Personal recognition techniques based on human iris recognition with waveform recognition", in Proceedings of the IEEE International Conference on Aerobics, Speech and Signal Processing (ICASSP '05), Vol. 2, pp. 949–952, Philadelphia, Pa, USA, March 2005.
[26] A. Hoover, v. Koznetsova, and M. Goldbom, "Detection of blood vessels in images of the retina by detecting the threshold of a matched filter response fragment," IEEE Transactions on Medical Imaging, vol. 19, No. 3, pp. 203–210, 2000.